Water, Energy, Food and Environment Journal
An International Journal

http://dx.doi.org/10.18576/wefej/030202

Functionalized CNT/PVDF Blended Flat Sheet Membrane for Water Desalination via Vacuum Membrane Distillation, Fabrication and Characterization

Elham El-Zanati[1], Esraa Taha[1], Reem Ettouney[2] and Mahmoud El-Rifai[2]*

[1]Department of Chemical Engineering and Pilot Plant, Engineering Research Division, National Research Centre, Dokki, Giza, Egypt.
[2]Departments of Chemical Engineering, Faculty of Engineering, Cairo University, Giza, Egypt.

Received: 21 Feb. 2022, Revised: 22 Mar. 2022, Accepted: 24 Mar. 2022.
Published online: 1 Jul 2022.

Abstract: The phase inversion procedure was used to prepare flat sheet membranes from polyvinylidene fluoride, PVDF. The impacts of casting solution composition, and exposure time on coagulation, were studied. For vacuum membrane distillation (VMD) of seawater desalination, PVDF flat sheet membranes with a novel sandwich structure and excellent wet resistance have been developed. The performance of the membrane was evaluated using an aqueous NaCl solution. At a temperature of 60°C for the feed and 16°C for permeate, a permeate flux of up to 21.24 lit/m2h were achieved. A salt rejection rate of more than 96 % was obtained in permeate. The water droplet had a contact angle with the membrane surface of 93^{o}.
CNTs were added as a hydrophilic agent to improve the membrane flux. PVDF membranes coated with carbon nanotubes are used in membrane distillation to provide superhydrophobic surfaces. These membranes showed high flux and excellent salt rejection, indicating will be used in desalination applications. Pore wetting, which has a negative effect on salt rejection, was improved, and the membrane stability was, improved with these modified membranes. The membrane modified with CNT/ODA had the maximum water flux (23 lit/m2.h) and high salt rejection (up to 98%). The water contact angle (WCA) of the coated membrane is, (108.4o). Scanning electron microscopy is used to examine all membrane structures. The porosity of the membranes ranged from 60 to 86 %.
Keywords: Polymeric Membranes, Water Desalination, Membrane Distillation, Nanoparticles, Enhanced Membrane.

1 Introduction

Water covers approximately 72% of the planet, the percentage of the salt water is about97%, and the accessible fresh water for human use is 3% of the total quantity. The challenge of supplying adequate and clean drinking water, which is aggravated by population increase, climate change, and industrialization revolution, has become one of the most pressing issues of our time[1]. People all around the world are attempting to tackle the problem through many pathways; as for instance desalination. As a result, it is important to investigate efficient and reliable desalination technologies[2].

Desalination of water can be accomplished using a variety of methods, the majority of them are based on selective membrane contacts, thermal distillation, and the use of electric fields. Primary thermal distillation (TD) techniques (such as multi-effect distillation(MED), multi-stage flash distillation (MSF), and thermal vapor compression), and the most attractive technology for producing fresh water from brackish water or seawater in membrane technologies is reverse osmosis (RO), however, its main disadvantage is flow restrictions due to fouling and scaling issues, as well as its relatively high energy consumption[3].

Correspondingauthore-mail: esraa.che13@gmail.com

Membrane distillation (MD) is being considered a viable alternative to the currently dominant RO desalination process. MD is a new technique for water desalination at moderate pressures and temperatures. A vapor pressure differential occurs when a temperature difference is maintained across the membrane. This driving force is created by heating the source water, which raises its vapour pressure above that of the desalted water collected as distillate on the opposite side, which is then cooled. As a result, liquid (typically salt water) evaporates at the hot interface, passes across the membrane as vapour, and condenses on the cold side, resulting in a net trans membrane water flux [1, 4].

MD provides various advantages over pressure-driven membrane processes, including high rejection for non-volatile components, lower operating pressure, significantly bigger membrane pore size, less sensitivity to fouling than RO, minimal sensitivity to feed salinity, low feed temperature requirements, and chemical pre-treatment of the water supply is not necessary[5, 6].

MD classed into four different configurations based on the condensation and vapour recovery, as well as the application of the driving force:(1) Direct contact membrane distillation (DCMD), (2) sweep gas membrane distillation (SGMD), (3) air gap membrane distillation (AGMD), and (4)vacuum membrane distillation (VMD)[7].

1) DCMD: The vapour is condensed by a liquid that is cooler than the feed and comes into direct contact with the permeate side of the membrane.
2) SGMD: The permeate vapour is transported via a gas stream.
3) AGMD: Before condensing on a nearby cold surface, the permeated vapour migrates across an air gap. Product water is condensed permeate that falls under gravity.
4) VMD: The vapour is towed by simple vacuum and then condensed in a separate apparatus if necessary.

Despite the fact that DCMD is the simple configuration, the VMD process has a large permeate flux under the same temperature gradient that, lower mass transfer resistance and zero conductive heat loss under a vacuum condition. The vacuum membrane distillation (VMD) method has the following advantages: it requires little plant space, operates at a low temperature, and produces low hydrostatic pressure. It also has moderate heat transmission on both the feed and permeate sides, does not require permeate side cooling, has low mass transfer resistance, and has low heat loss [8].

VMD is an evaporative process using porous and hydrophobic membranes. Membranes used in MD are fabricated from polytetrafluoroethylene (PTFE), polypropylene (PP), and polyvinylidene difluoride (PVDF) [9, 10]. The averages of pore diameter, membrane porosity, and thickness determine the flow rate across the membrane pores. Additives can be dissolved in the polymer casting solution to create membranes with a special properties [11]. These additives are used to build a spongy membrane structure and prevent macro voids from forming.

Flat sheet and Hollow Fiber (HF) membranes are widely used in water desalination by VMD [12]. To enhance VMD membrane performance, nanoparticles (CNT, GO, TiO2, Al2O3, ……etc) can be added as an additive into the polymer dope solution or as a coating material on the prepared membrane surface. They are used to improve the mechanical strength of polymer-based membranes as well as the other functional properties of the membranes [13]. Besides, nanomaterials with specific properties can be obtained by thermal and/or chemical modification [14][15].

CNTs are considered an alternative in modifying the structures and improving the performance of the currently used MD membranes. CNTs enhanced the overall performance of the membrane used in VMD [16]. One of the powerful techniques is the use of CNTs in membrane surface chemistry. As an environmentally friendly approach, and versatile, spray coating has been broadly utilized in fabricating super hydrophobic surfaces. It has additionally been utilized in manufacturing hydrophobic membranes with CNTs [17]. In the membrane surface, CNTs enhanced water vapor delivery potential and increased hydrophobicity. Many methods for fabricating CNTs-based hydrophobic membranes have been proposed, including phase inversion, surface coating, and chemical grafting [18][19].

The article is aiming at prepare, develop, and describe enhanced hydrophobic porous membranes, as well as, aiming at assessing their performance in a VMD process under various operating conditions. A hydrophobic (PVDF) membrane was fabricated using CNTs to construct blended, functionalized, and coated membranes, as well as to investigate alternative CNT compositions to improve membrane permeability. The membranes prepared from the CNT/PVDF blended and functionalized with octadecyl amine (ODA), those membranes were tested in the VMD system, and the performance was obtained in terms of salt rejection and water permeation of salty water. This can

effectively improve the hydrophobic surface of the membrane, and increase membrane porosity to enhance water vapor permeability.

2 Experimental

2.1 Materials

A commercial polyvinylidene fluoride (PVDF) powder, the polymer used in this study, was supplied by Alfa Aesar Inc (Germany). 1-Methyl-2-Pyrrolidinone (NMP), 99% purity was used as the solvent without any further purification; (SigmaAldrich, USA). Lithium chloride (LiCl), 99% purity, was used as a modifying agent as a non-solvent additive to the casting solution (Alpha Chemicals Company,India). Ethylene glycol (EG), as a performing additive, Assay 99%, (Fisher Chemicals Company, Canada). Carbon Nanotubes, 95% purity, D=10-40 nm, L=20μm, density 1.3- 2.4 g/cm3 specific surface area 460 m2/g (ORCHID, Nanometals Company, Egypt). Sulfuric acid(H2SO4) 97%, was used as a pure reagent for analysis, (ADWIC, Egypt), Nitric acid (HNO3) 98%, (Fisher, United Kingdom) and Octadecyl amine (ODA), technical grade 90%, was purchased from ALDRICH (Japan). Anhydrous ethanol, 99.8% purity, (Piochem Company, Egypt).

2.2 Preparation of unmodified membrane (M0)

The PVDF polymer dope solution was prepared by adding PVDF, EG, and LiCl into NMP with a weight ratio of 15/3/5/77, respectively. The mixture was mechanically stirred for 4 hr at 65 °C until a homogeneous solution was formed. After complete dissolution, the dope mixture was continuously stirred at a low speed to prevent any sedimentation. The dope solution was degassed overnight before being cast. The polymer solution was then the cast with a thickness of 400 μm on a glass plate and immediately immersed into a water-coagulating bath. After one day, the precipitated membrane was removed from the coagulation bath. The resultant membrane was then dried in air for one day.

2.3 Preparation of blended membrane with Pristine CNT

Surface modification of the M1 membrane was accomplished using a solvent evaporation-type phase inversion method to create a porous selective layer on the membrane surface. Polymer dopes were prepared by adding CNT particles into M0 dope solution with different weight percentages: 0.01, 0.05and 0.1. The casting solution was prepared by initially sonicating (ultrasonic processor UP200Ht, Hielscher Co., Taiwan) the suitable amount of nanoparticle CNT in solvent NMP and, then adding additives LiCl, EG, and polymer PVDF to this suspension. To achieve optimal particle dispersion, the mixture was then agitated at 65°C until it was homogenous. The polymer solutions were kept overnight to remove air bubbles. To form a membrane, the polymer solution was cast at room temperature onto a glass plate using a casting knife (Hasco Co., Egypt), after that, the membrane was immersed in a coagulation bath containing distilled water. The composition of the dope solution is presented in Table (1).

Table 1: Dope solution compositions.

Membrane Code	CNT, wt%	PVDF, wt%	LiCl, wt%	EG, wt%	NMP, wt%
$\mathbf{M_0}$	0	15	5	3	77
$\mathbf{M_1}$	0.01	15	5	3	77
$\mathbf{M_2}$	0.05	15	5	3	77
$\mathbf{M_3}$	0.1	15	5	3	77

2.4 Functionalization of CNT with Octadecyl amine (ODA) to prepared modified membrane

The synthesis of carboxylated CNTs (CNT–COOH), was carried out as follows. CNTs, were prepared by improved Hummer's method [20]. To make the CNTs easier to distribute in the organic solvent, they were surface modified with concentrated acids, namely nitric acid and sulfuric acid (1:1 in vol.%). 0.3 g of raw CNT was added to 20 ml of the acid mixture in a stainless-steel closed vessel and put in a vacuum oven (vacuum dryer oven, DFA-7000, china) at 200^{o}C for 3 h. The vessel was allowed to cool in the air at room temperature after the heat treatment. To eliminate the excess acid, the recovered CNTs were rinsed many times with distilled water until a neutral pH, was achieved. After cooling and washing, the product was filtered using filter paper, and then the samples were dried overnight at

room temperature. This led to the formation of carboxylated CNTs (CNT–COOH) which, were characterized by FTIR to confirm the presence of carboxyl groups.

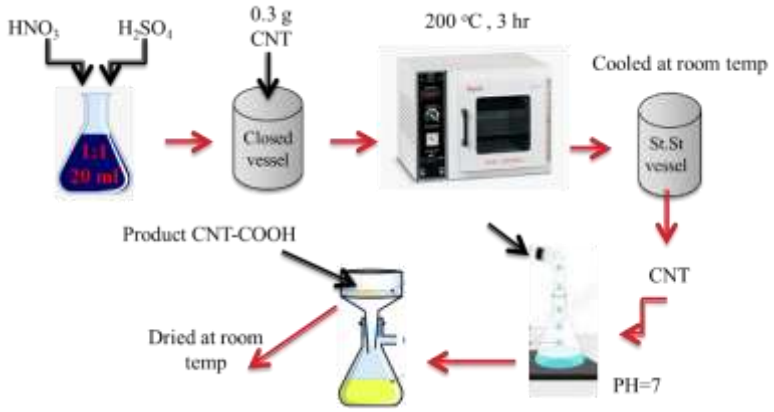

Fig. 1: Carboxylated CNTs (CNT–COOH) by Hummer's method.

To synthesize a new super-hydrophobic nanoparticle (CNT-NH2) functionalization of CNT was carried out. The first 170 mg of prepared powder was dispersed in 100 ml of ethanol for 30 min using an ultrasonicator. Then, 700 mg of ODA was gradually added to the solution and sonicated for 2 hours. The obtained CNT-ODA was vigorously stirred at 40oC for 1 h and dried at 120°C for 1 h in a vacuum oven. Finally, CNT-ODA was redispersed in ethanol and filtered to create a superhydrophobic surface of CNT-ODA [21, 22]. Figure 3 shows a schematic representation of the functionalization process. Polymer dope was prepared by adding CNT-ODA particles into M0 dope solution with 0.05% by weight (M2f) by using the same previous procedure.

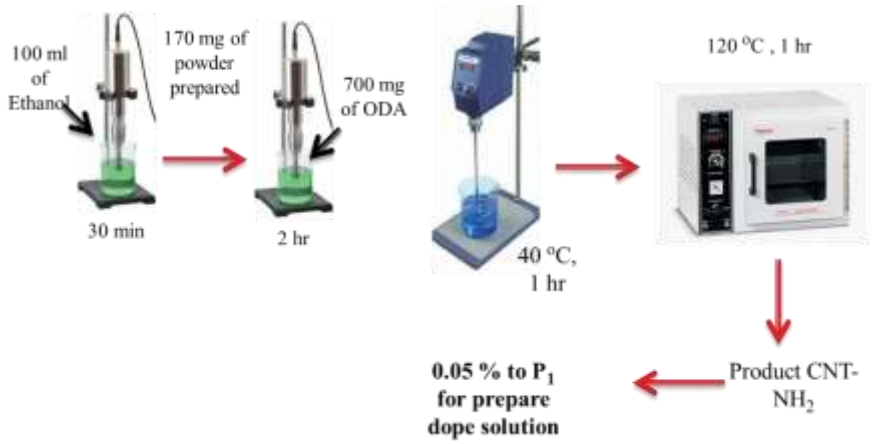

Fig. 2: Functionalization of CNTs (CNT – NH2).

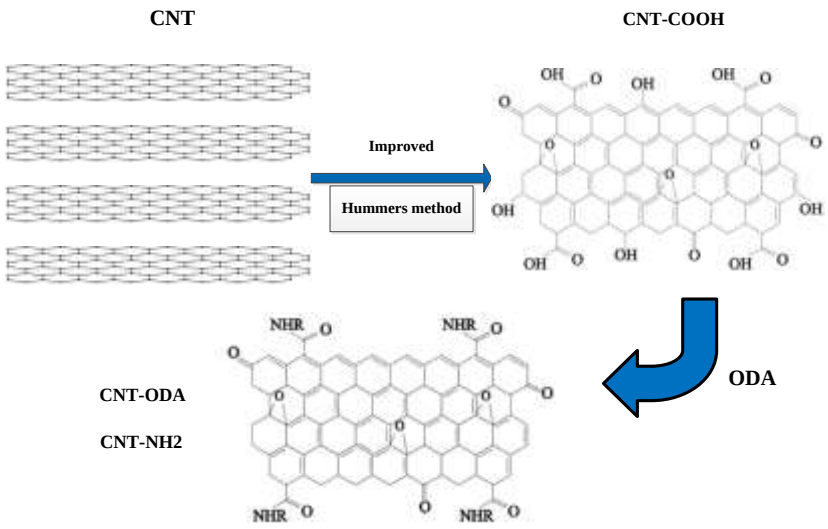

Fig.3: Schematic for the mechanism of functionalization of CNT with octadecyl amine.

2.5 Characterization of membranes

The membrane morphology and surface topography were studied using SEM ((JEOL 5410), 20 kV). The dry membrane samples were cut into 0.5 cm long sections and gold-sputtered for electrical conductivity [7]. The contact angle device (model OCA 15EC), which was fabricated by the company Data Physics Instrument Gmbh and equipped with an image processing program with a sessile drop method, was used to measure the contact angle, which is typically employed to determine the hydrophobicity of membrane surfaces. Water droplets were dropped onto the membrane surface to be assessed. The photos were acquired at a rate of 12 frames per second by a mounted motion camera. The contact angle was, determined by using the Attention software to measure the recorded footage. Each sample's contact angle data was, calculated using an average of five readings [23]. The gravimetric approach was used to calculate the membrane porosity. Ethanol was used to completely moisten the membranes. After the leftover ethanol on the surface was evaporated, the weight (w_1, g) of the wetted membrane was measured. After being left in the open air for 15 minutes, the membrane samples were dried and weighed (w_2, g). The porosity was measured using the aforementioned equation (1), where ρ_p: The density of the PVDF (g/m^3) and ρ_e: The density of the ethanol (g/m^3) [6].

$$\varepsilon m = \frac{(w1-w2)/\rho e}{\frac{w1-w2}{\rho e}+w2/\rho p} \times 100 \qquad (1)$$

The vibrational spectrum of a molecule is regarded as an unparalleled physical characteristic. As a result, by comparing an unknown spectrum to previously recorded reference spectra, the infrared spectrum can be utilized to identify materials. The PVDF phases of the virgin and treated membranes were investigated using a Fourier-transform infrared (FT-IR) spectroscope (Burker vertex 70). Each spectrum was obtained in transfer mode by pressing the sample with KBr on a pellet, with a signal averaging 4000-400 cm-1 scans at a resolution of 4 cm-1. Transparent films were created using infrared (IR) cards [24].

2.6 Evaluation of membrane performance by VMD

The prepared membranes were evaluated and assessed for application as hydrophobic porous membranes used in membrane distillation systems in the existing VMD unit at the National Research Centre (Figure 4). The flat sheet membranes were tested using modules having a diameter of 11.5 cm. Batches of 2L with different percentages of NaCl solution were used as the feed. The feed had a temperature of 65°C with a volumetric flow rate of 18cm^3/sec. The permeate side of the membrane was connected to a vacuum pump with a pressure of about 1 bar (absolute pressure 0 bar). The permeate was condensed and collected in a glass bottle, and the permeate volume and salinity were measured. The water permeation flux (J) was determined using the equation below (2):

$$J = \frac{M}{A \times t} \qquad (2)$$

Where J is the permeate flux, lit/ (m^2·hr), M is the volume of distilled water, lit, A is the membrane area, m^2, and the time, h.
Salinity was measured by an EC/TEMP meter (AD 8000, Adwa instrument, Romania). The salt rejection was recorded at different salt concentrations of feed and permeate. The salt rejection (SR) was obtained using the following expression Eq. (3), where C_P; the final salt concentration of the permeate stream andC_F; the initial salt concentration of the feed. The salt rejection (SR) was determined using the equation below (3):

$$SR = \frac{Cf - Cp}{Cf} \times 100\ \% \qquad (3)$$

The MD test for promising samples M_0, M_1, M_2, M_3, and M_{2f} was tasted for verification. The permeation flux and salt rejection were calculated for all membranes. The average values for the results of experiments were taken.

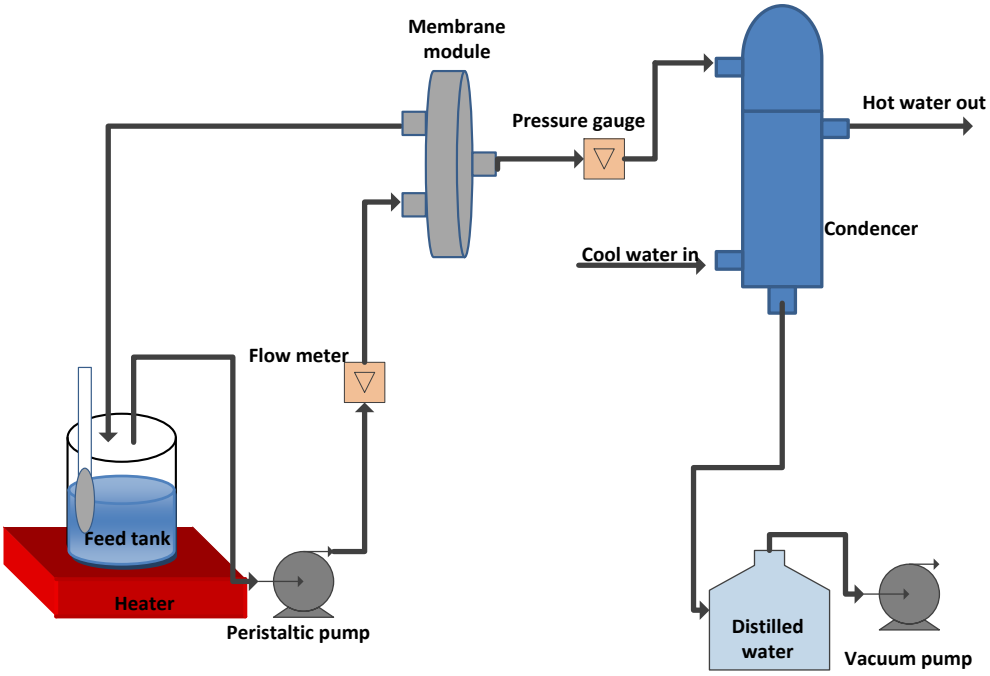

Fig.4: Schematic diagram of the VMD experimental setup.

3 Results and Discussion

3.1 Characterization of membranes

3.1.1 Scanning electron microscopy (SEM)

The top surface and cross-sectional SEM images of different membranes produced are shown in Figure 5. Under a magnification of 20k, the layer surface is microporous. Water vapour movement through the membrane is harmed as a result of this. The second layer, on the other hand, is completely permeable [25]. This is useful because it lowers the resistance to vapour movement during VMD. As a result, the membrane shows a VMD permeation flux of 21.2 lit/m2h and salt rejections of 96.85 %.

The top surface of the unmodified membrane is shown in Figure 5 (a). It has a porous structure with more pores. Figure 5 (b) is the cross-section of the membrane revealing more pores. M_0 had a finger-like void structural layer and a sponge-like structural layer. This phenomenon can be explained as follows: The non-solvent-induced time was zero when the membrane was immersed in a water bath directly, so rapid interchange between water and

NMP favored the formation of a finger-like structure on the upper layer, whereas delayed demixing favored the formation of a sponge-like structure on the lower layer. The solvent in the membrane was gradually absorbed into the surface of the liquid film when it was placed in a water coagulation bath [26].

The top surfaces and cross-section CNTs/M_0 blended membranes are shown in Figure 5(c, d, e, f, g, and h). With increasing pore size, the membrane surface grew rougher. The M_2 membrane, which contains 0.05 wt.% CNTs, appears to have the roughest surface and the largest pore size. These images reveal that the M_2 membrane has a modular structure with increased pore size and a rough surface due to the hydrophilic functional groups on the CNTs. The rapid exchange of non-solvent and solvent by hydrophilic CNTs during the phase inversion process could explain this outcome [27].

However, as the CNT concentration grew, particularly at 0.1 wt. percent, the surface structure began to smooth out again. This could be owing to the M_3 blend solution higher viscosity. As previously stated, the viscosity of the blend solutions increased as the amount of CNTs increased. The creation of the microporous mix membranes was influenced by two factors: enhanced hydrophilicity and higher viscosity due to the addition of hydrophilic CNTs. Increased hydrophilicity of the solution caused the nodular structure when the concentration of the additional CNTs was less than 0.1 wt. %, whereas increased solution viscosity was the major factor for a smooth membrane surface when it was more than 0.1 wt.%.

The surface morphology and cross-section of CNT-ODA/M_0 are shown in Figure 5 (i, j) respectively. The cross-sectional structure of the modified membrane shows that channels from CNT cleared, and compared it with an unmodified membrane (M_0) and unfunctionalized CNT(M_2), the thickness of the modified membrane decreases. M_{2f} membrane displays a similar morphology with cavities originating from the substrate inside the membrane. There is a difference between modified (M_2f) and unmodified (M_0, M_2) membranes on the surface image, and the modified membrane pore size reduced after modification.

During the phase inversion process, the unmodified membranes have a loose and smooth surface with a sponge-like and porous structure inside the membrane with lower cavities [19]. The modified membrane surface structure is bumpy, dense, and full of cavities, and CNT-ODA nanoparticles are dispersed asymmetrically across the membrane. Furthermore, pores in the modified membranes are found at the membrane surface regions.

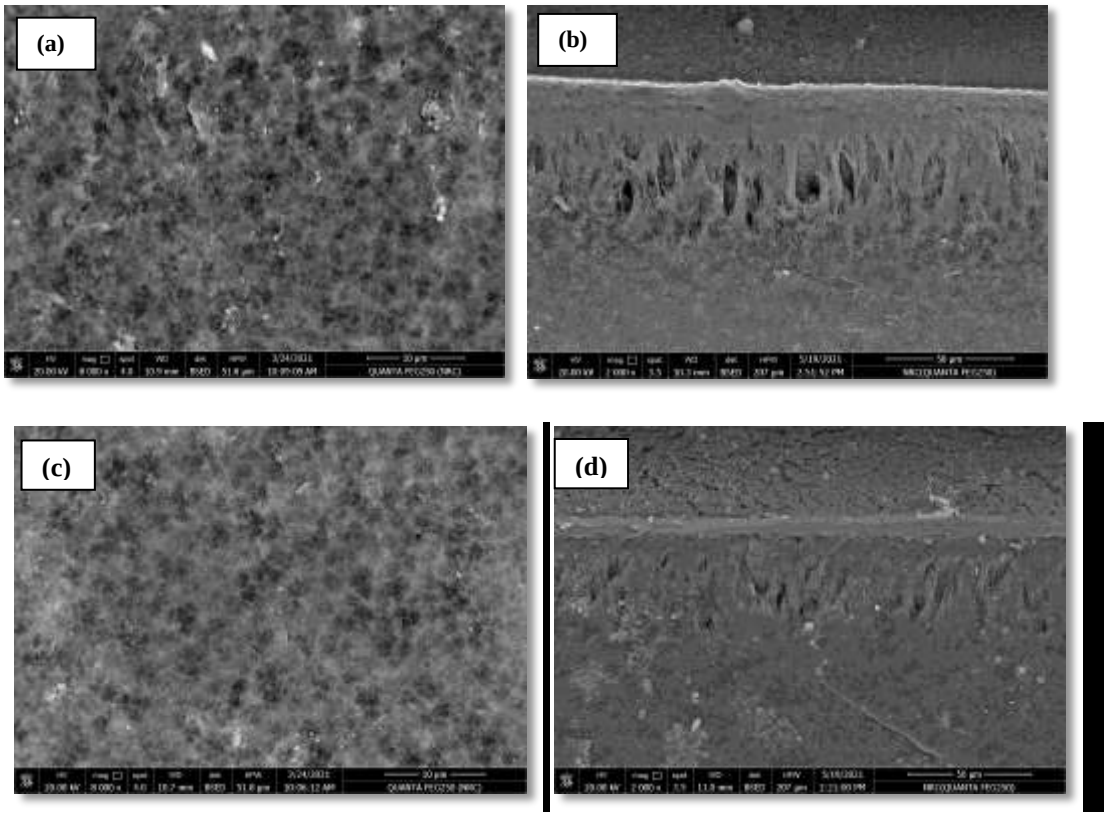

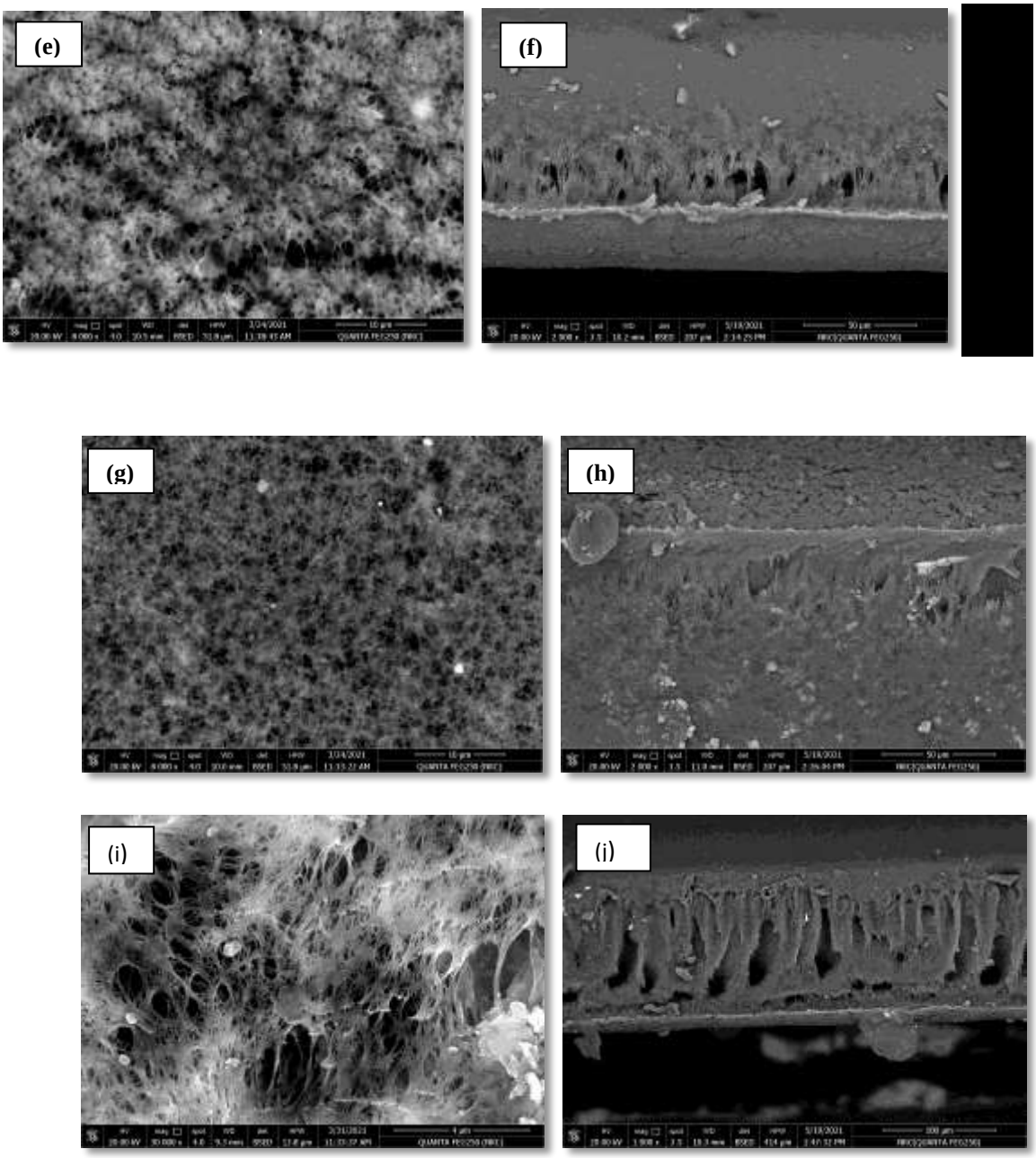

Fig. 5: SEM morphology of the top surface and cross section of the unmodified, blended membranes and modified membrane with ODA: (a, b) M_0, (c, d) M_1, (e, f) M_2, (g, h) M_3, (i, j) M_{2f}

3.1.2 Hydrophobicity of membranes (CA)

The hydrophobicity of all prepared membranes was investigated by CA measurement as shown in Figure 6. The CA of the water at the top surface of unmodified membrane M0 was 93.9 o as shown in Figure 6 (a), high enough to keep hot water out of entering the membrane pores [28].

The contact angle increases with increasing CNTs up to a value of 0.05%. This gave the largest CA of 81.6. Beyond 0.05% CNT is associated with a decrease in CA. This means that the hydrophilic CNTs transported to the membrane surface during the phase inversion process in water, making the surface of the membrane hydrophilic. As

illustrated in Figure 6, increasing the CNT content makes the membrane surface hydrophilic and supports the decreasing contact angle.

The CNT-ODA added to the PVDF membrane was also observed to impact the surface hydrophilicity of the modified blended membrane. As a function of the contents, Figure 6 shows the contact angle of the act and the surfaces of the blended membranes. The CNT-ODA gave a contact angle (CA) higher than the CA of the CNT blended membrane without functionalization as shown in Figure 6 (c). The water contact angle (WCA) of M_2f = 108.4^o is higher than the WCA of M_2 = 81.6^o. The functionalized CNT in a polymer solution is better than adding pristine in both performance and characterization. The presence of CNT-ODA in the modified membranes, which generated interconnecting nano-channels with large surface area for high NaCl rejection and fast water flow, was attributed to the improved membrane performance [29]. It is seen that the CA of the M_{2f} membrane is higher than other membranes; indicating that the hydrophobicity of the M_{2f} membrane is higher than others [26].

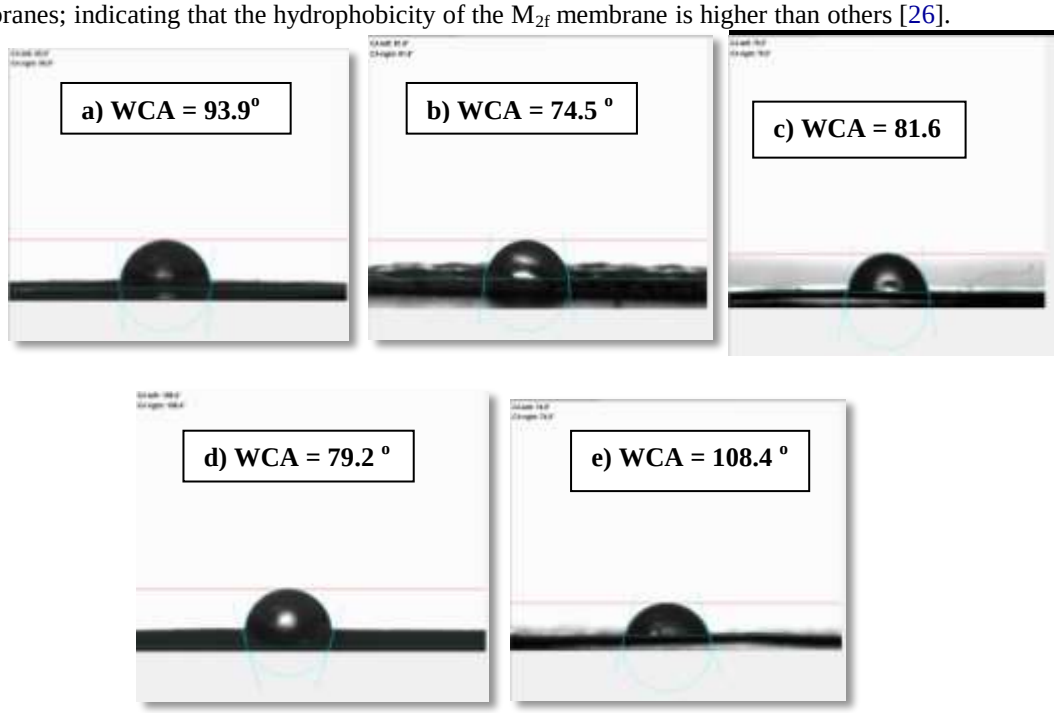

Fig. 6: Contact angles on the unmodified membrane, blended membranes and modified membrane: (a) M_0, (b) M_1, (c) M_2, (d) M_3, and (e) M_{2f}

3.1.3 Fourier transform-infrared spectroscopy (FT-IR)

Figure 7 presents the FT-IR spectra of CNT, CNT-COOH, and CNT-ODA. The pure CNT was divided into the following functional groups Figure (7 a): In the range of 3200–3550 cm^{-1}, and specifically at 3431 cm^{-1}, the large and strong O-H stretching vibration band was found. C=C stretching of conjugated alkenes, which emerges between 1620 and 1680 cm^{-1}, is thought to be responsible for the peak at 1648 cm^{-1}. In addition, the peak at 1408 cm^{-1} is associated with -OH carboxyl, the band at 1278 cm^{-1} with C-O-C epoxy, and the peak at 1089 cm^{-1} with C-O alkoxy [19, 20, 30].

In Figure (7 b), the treated CNTs shows –COOH and –OH functional groups. C=O and –OH stretching correlate to the peaks at 1729 and 3466 cm^{-1}, respectively, confirming the presence of carboxyl groups in the modified CNTs. Conjugation of C=O with C=C bonds or interaction between localized C=C bonds and carboxylic ketenes and acids are expected to cause the peaks between 1312 and 1465 cm^{-1}.The peaks between 2852 and 2970 cm^{-1} are linked to the stretching vibrations of C–H [27, 31].

The peaks at 1654 cm^{-1} and 3437 cm^{-1} in the spectra of CNT-ODA Figure (7 c) are attributable to (C=O stretching) of amide groups and (N-H stretching), respectively. On CNT-ODA, the peak at 704 cm^{-1} corresponds to the octadecyl chain –CH2 stretching. The new peak in the CNT-ODA at 1461 cm^{-1} (N-H stretching) confirms the

interaction between ODA molecules (amine groups), and CNTs (epoxy groups). The vanishing of the peak at 1729 cm^{-1} (carboxyl groups) in CNT indicates that ODA combines with CNT carboxyl groups as well as epoxy groups to create secondary amines. It is also worth mentioning that the interaction between ODA and CNT includes nucleophilic substitution between epoxy and amine, electrostatic attraction between protonated amine and carboxylic groups of CNT, and hydrogen bonding between amine and oxygen-containing functional groups of CNT, but the nucleophilic substitution reaction is the basic reaction [19, 30].

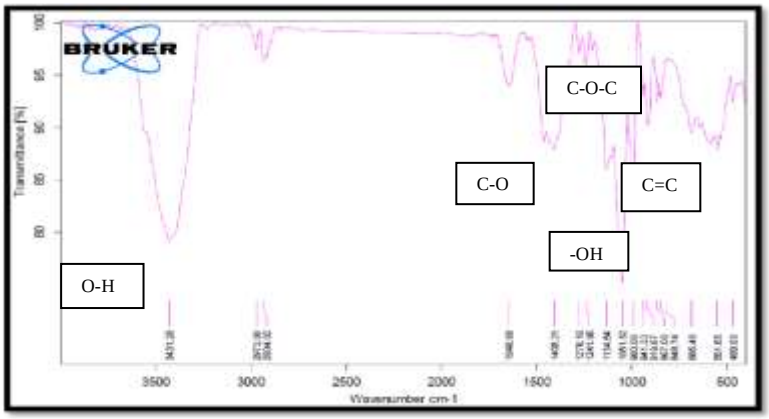

(a) CNT pristine powder

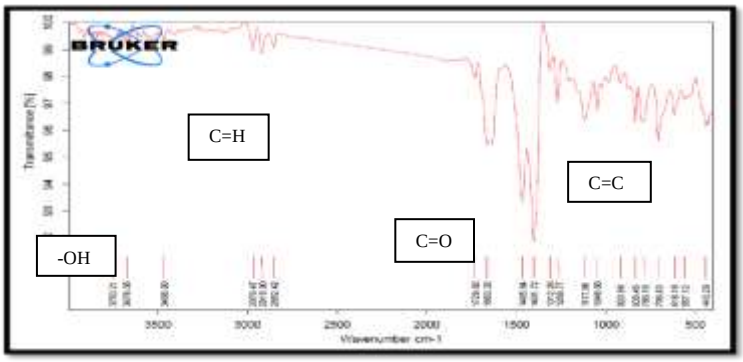

(b) Acid treated CNTs

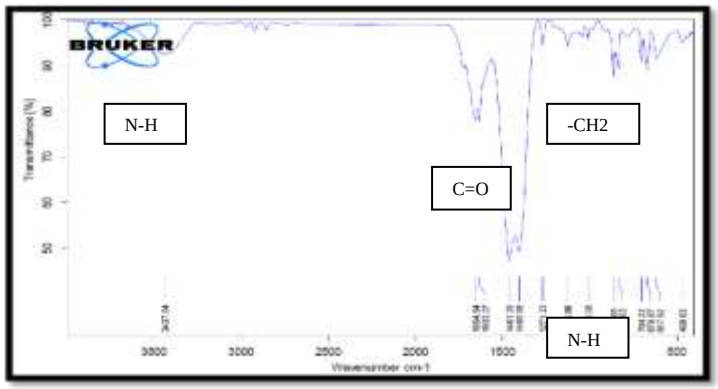

(c) CNT-ODA

Fig.7: FTIR spectra of (a) CNTs pristine, (b) acid treated CNTs, (C) CNT-ODA.

3.1.4 Porosity and membrane thickness

Water vapour flux in MD membranes is significantly related to membrane porosity and thickness. Table (2) shows the porosity and thickness of all prepared membranes. By increasing membrane porosity, the amount of vapour transferred through the membrane rises. Reduced membrane thickness, on the other hand, provides less resistance to vapour movement through the membrane. Table (2) shows that the porosity of all membranes used is quite high, and ranges from 75% to 82%. M3 has a greater porosity due to the amount of CNT additive added to the dope solution, which affect fibers morphology [7].

Table 2: Porosity and thickness for all membrane prepared.

	ϵ %	Thickness, mm
M0	82%	0.062
M1	80%	0.012
M2	81%	0.05
M3	82%	0.086
M2f	75%	0.04

3.2 Membrane performance evaluation

The membrane requirements for membrane distillation are high flux and high salt rejection (SR). The feed temperature is the main operating parameter that significantly affects the MD flux, due to the increase in the vapor pressure with temperature. This type of dependence has been thoroughly investigated in several studies [26]. To evaluate the VMD performance of a flat sheet membranes were tested. Table (3) elucidates the permeate flux and salt rejection of flat sheet membranes prepared.

The unmodified membrane M_0 show the high membrane water vapor flux (21.2 lit/m^2.h) and high salt rejection (96.85 %). The blended membranes with addition of different CNT wt.% M1, M2 and M3. The membrane distillation flux increased, as can be observed. The highest value was obtained at 0.1 wt% CNT, the blended membrane reached a maximum membrane distillation flux of about 22.6 lit/m^2h. The increased permeate flux was attributable to the unique surface features of CNTs, which offered improved adsorption and quick desorption [15]. The salt rejection of all membranes is decreased to (83%).

The modified membrane CNT-ODA (M_{2f}) produced a greater flow from MD at 60^{o}C than the unmodified membrane M_0. Flux reached 22.6 lit/m^2.h for M_2f membrane and 21.2 lit/m^2.h using M_0 membranes, with salt rejection results for M_2f higher than M_0 reaching 98.1% while M_0 reached 96.9%. Comparison between adding 0.05% CNT in polymer solution without modification (M_2) and with modification (M_2f) revealed that M_2f is higher than M_2 with a 29.5% increase in flux and a 14.7% increase in SR.

Table 3: VMD results for different prepared membranes saline water as feed (P vacuum 1bar, Tf 60Oc.

	Collected, ml	Time, min	Flux, lit/m^2.hr	salt in	salt out	SR%
M_0	60	15	21.2	17.5	0.55	96.85
M_1	45	20	11.9	40	6.8	83
M_2	60	20	15.9	60	9.8	83.67
M_3	85	20	22.56	45	8	82.2
M_{2f}	85	20	22.57	50	0.96	98.08

4 Conclusions and Future trends in the field

To improve pure water flux in membrane distillation, carbon nanotubes (CNTs) were inserted into PVDF membranes. The desalination performance of the CNT-enhanced membrane was consistently better than that of the standard membrane. The modified membrane with CNT-ODA, the permeate flux reached the highest value of 23 lit/m^2 h and the salt rejection was greater than 98%. These findings suggest that CNTs improved vapor permeability while preventing liquid permeation into membrane pores via altering water-membrane interactions. The membranes were stable for extended periods of time with no salt leakage.

Anti-wetting membranes with high water repellency should be prepared to improve membrane stability in long-term MD operation to increase vapor flux, and improve permeate quality. At the lab scale, significant desalination performances have been achieved using certain filler materials (such as CNTs, graphene and its derivatives, TiO_2, silica). It is worth noting that choosing the proper additive can have various advantages and could be the key to obtaining membranes for a large-scale procedure. Laboratory-scale investigations have received the most of the attention thus far. This could be owing to the high cost of new nanofillers such graphene and CNT. Less expensive alternatives should be chosen that have the same effect on the membrane.

Furthermore, given the major shortcomings of MD membranes (such as fouling, wetting, stability, heat and mass transfer, and resistances), that should concentrate on developing the next-generation of membranes that can meet all of the requirements for true seawater desalination. The ability to use MD for seawater desalination or industrial wastewater reclamation with low-surface-tension pollutants is enabled by the creation of nano-scale surface morphology with air pockets. Reentrant structure, in addition to high hydrophobicity and low solid/liquid interface energy, is critical in achieving omniphobic characteristics in a membrane, allowing for strong repellence against liquids with a wide range of surface tensions. As a result, omniphobic membranes appear to hold promise for real-world seawater desalination.

References

[1] Edwie, F., M.M. Teoh, and T.-S. Chung, *Effects of additives on dual-layer hydrophobic–hydrophilic PVDF hollow fiber membranes for membrane distillation and continuous performance.* Chemical Engineering Science, 2012. **68**(1): p. 567-578.

[2] Rastegarpanah ،A. and H.R. Mortaheb, *Surface treatment of polyethersulfone membranes for applying in desalination by direct contact membrane distillation.* Desalination, 2016. **377**: p. 99-107.

[3] Zuo, J., et al., *Hydrophobic/hydrophilic PVDF/Ultem® dual-layer hollow fiber membranes with enhanced mechanical properties for vacuum membrane distillation.* Journal of Membrane Science, 2017. **523**: p. 103-110.

[4] Zhang, J., et al., *Fabrication and characterization of superhydrophobic poly (vinylidene fluoride) membrane for direct contact membrane distillation.* Desalination, 2013. **324**: p. 1-9.

[5] Silva, T.L.S., et al., *Multi-walled carbon nanotube/PVDF blended membranes with sponge- and finger-like pores for direct contact membrane distillation.* Desalination, 2015. **357**: p. 233-245.

[6] Pagliero, M., et al., *Novel hydrophobic PVDF membranes prepared by nonsolvent induced phase separation for membrane distillation.* Journal of Membrane Science, 2020. **596**: p. 117575.

[7] Drioli, E., et al., *Novel PVDF hollow fiber membranes for vacuum and direct contact membrane distillation applications.* Separation and Purification Technology, 2013. **115**: p. 27-38.

[8] El-Zanati, E., et al., *Development of vacuum multi-effect membrane distillation system of pilot-scale for water desalination.* Desalination and Water Treatment, 2021. **217**: p. 22-30.

[9] Li, Z., et al., *Electrospun polyvinylidene fluoride/fluorinated acrylate copolymer tree-like nanofiber membrane with high flux and salt rejection ratio for direct contact membrane distillation.* Desalination :466 .2019 ،p. 68-76.

[10] Kang, G.-d. and Y.-m. Cao, *Application and modification of poly(vinylidene fluoride) (PVDF) membranes – A review.* Journal of Membrane Science, 2014. **463**: p. 145-165.

[11] Abdallah, H., et al., *Hydrophobic polyethersulfone porous membranes for membrane distillation.* Frontiers of Chemical Science and Engineering, 2016. **9**(1): p. 84-93.

[12] Pichardo-Romero, D., et al., *Current Advances in Biofouling Mitigation in Membranes for Water Treatment: An Overview.* Processes, 2020. **8**(2): p. 182.

[13] Acarer, S., et al., *Manufacturing and Characterisation of Polymeric Membranes for Water Treatment and Numerical Investigation of Mechanics of Nanocomposite Membranes.* Polymers (Basel), 2021. **13**.(10)

[14] Bhadra, M., S. Roy, and S. Mitra, *Enhanced desalination using carboxylated carbon nanotube immobilized membranes.* Separation and Purification Technology, 2013. **120**: p. 373-377.

[15] Ragunath, S., S. Roy, and S. Mitra, Carbon nanotube immobilized membrane with controlled nanotube *incorporation via phase inversion polymerization for membrane distillation based desalination.* Separation and Purification Technology, 2018. **194**: p. 249-255.
[16] Xie, B., et al., *Engineering carbon nanotubes enhanced hydrophobic membranes with high performance in* membrane distillation by spray coating. Journal of Membrane Science, 2021. 625: p. 118978.
[17] Obotey Ezugbe, E. and S. Rathilal, *Membrane Technologies in Wastewater Treatment: A Review.* Membranes (Basel), 2020. **10**.(5)
[18] Rashed, A.O., et al., *Carbon nanotube membranes – Strategies and challenges towards scalable manufacturing and practical separation applications.* Separation and Purification Technology, 2021. **257**: p. 117929.
[19] Zahirifar, J., et al., *Fabrication of a novel octadecylamine functionalized graphene oxide/PVDF dual-layer flat sheet membrane for desalination via air gap membrane distillation.* Desalination, 2018. **428**: p. 227-239.
[20] Yuan, X.T., et al., Multifunctional PVDF/CNT/GO mixed matrix membranes for ultrafiltration and fouling detection. J Hazard Mater, 2020. 384: p. 120978.
[21] Liu ،H.-d., et al., Superhydrophobic property of epoxy resin coating modified with octadecylamine and SiO2 nanoparticles. Materials Letters, 2019. 247: p. 204-207.
[22] Bhadra, M., S. Roy, and S. Mitra, A Bilayered Structure Comprised of Functionalized Carbon Nanotubes for Desalination by Membrane Distillation. ACS Appl Mater Interfaces, 2016. 8(30): p. 19507-13.
[23] Das, R., et al., Carbon nanotube membranes for water purification: A bright future in water desalination. Desalination, 2014. 336: p. 97-109.
[24] Dhatarwal, P. and R.J. Sengwa, Tunable β-phase crystals, degree of crystallinity, and dielectric properties of three-phase PVDF/PEO/SiO2 hybrid polymer nanocomposites. Materials Research Bulletin, 2020. 129: p. 110901.
[25] Zuo, J. and T.-S. Chung, PVDF hollow fibers with novel sandwich structure and superior wetting resistance for vacuum membrane distillation. Desalination, 2017. 417: p. 94-101.
[26] Fan, H., et al., Preparation and characterization of hydrophobic PVDF membranes by vapor-induced phase separation and application in vacuum membrane distillation. Journal of Polymer Research, 2013.(6)20 .
[27] Choi, J.-H., J .Jegal, and W.-N. Kim, Fabrication and characterization of multi-walled carbon nanotubes/polymer blend membranes. Journal of Membrane Science, 2006. 284(1-2): p. 406-415.
[28] Qtaishat, M., M. Khayet, and T. Matsuura, Novel porous composite hydrophobic/hydrophilic polysulfone membranes for desalination by direct contact membrane distillation. Journal of Membrane Science, 2009. 341(1-2): p. 139-148.
[29] Kyoungjin An, A., et al., Enhanced vapor transport in membrane distillation via functionalized carbon nanotubes anchored into electrospun nanofibres. Sci Rep, 2017. 7: p. 41562.
[30] Fouladivanda, M., et al., Step-by-step improvement of mixed-matrix nanofiber membrane with functionalized graphene oxide for desalination via air-gap membrane distillation. Separation and Purification Technology, 2021. 256: p. 117809.
[31] Chen, Y., Z. Iqbal, and S. Mitra, *Microwave-Induced Controlled Purification of Single-Walled Carbon Nanotubes without Sidewall Functionalization.* Advanced Functional Materials, 2007. **17**(18): p. 3946-3951.